A Microscope Image Auto-Focus Method Based on Colorful-Gradient

Po-Yi Li[1], Chia-Jen Liu[2], Cheng-Kuan Lin[3,*] and Yu-Chee Tseng[3]

[1]*Department of Biological Science and Technology, National Yang Ming Chiao Tung University, Taiwan*

[2]*Institute of Emergency and Critical Care Medicine, School of Medicine, National Yang Ming Chiao Tung University, Taiwan*

[3]*Department of Computer Science, National Yang Ming Chiao Tung University, Taiwan*

Abstract: Blood testing has always been an important indicator for judging patients' states and various types of lesions. The typical way to observe the blood sample is by having medical personnel operate the conventional microscope and classify the white blood cells in a patient's blood sample. However, such a long period of observation may cause visual fatigue. As a result, we built an automated microscope system to ensure the efficiency of the observation. In addition, focus measurement has always been a huge topic in the auto-focus method, which we implemented in the system. We proposed an automatic focus algorithm based on the gradient operator and colorfulness value to fit with the automated microscope system. The color-gradient operator is compared to conventional operators such as Laplacian-based, Wavelet-based, and DCT energy-based. By taking advantage of the three components in the color-gradient operator, the standard of determining a microscope image consists of both sharpness and colorfulness. The experimental results showed that the proposed microscope automatic focus algorithm is significantly stable in all real-life blood cell microscope image dataset scenarios. Such performance is discussed in specific situations that happened only in microscope auto-focus measurements.

1 INTRODUCTION

Clinically, blood testing has always been one of the critical indicators for judging the state of patients and various types of lesions. For example, by counting and classifying white blood cells in a patient's blood sample, you can know whether the patient has leukemia and the type of leukemia. In addition, various indexes of white blood cells are also closely related to Covid-19. In 198 COVID-19 patients, the research of Tong et al. shows that the survivors' lymphocytes, basophils, and eosinophils levels were significantly higher than those of non-survivors (Tong et al., 2021). Blixt et al. observed that the most convalescent COVID-19 patients have robust and durable B and T cell immunity (Blixt et al., 2022). Therefore, improving the detection efficiency and accuracy of white blood cells is very important, which will help to judge the patient's status accurately.

In the field of leukemia-related disease, acute myeloid leukemia (AML) accounted for a large proportion. Practically, medical personnel spends hours of microscope observation on patients' blood sample to identify their health. However, looking straight into the microscope for hundreds or even thousands of samples often cause visual fatigue or lower overall efficiency. Therefore, many manufacturers of microscope accessories have launched series for automatic photography to solve the fatigue of repetitive operation behavior. Taking the Lionheart LX/FX series of automated microscopes launched by BioTek as an example, it costs about 40,000 to 70,000 US dollars per device. Nonetheless, the whole product line of the digital microscope DM B series launched by Leica also costs about 5,000 to 10,000 US dollars. As we can see, although the fatigue problem of medical personnel has been solved at first glance, such an automated photographic microscope is too expensive for many medical institutions with relatively insufficient funds.

To solve the problems which people met in real life, we came up with the idea of building an automated photography microscope system having the following features: (1) modulized structure, (2) lower price, (3) ability to analyze the image. The main idea is to build a retrofit modular system that can easily in-

---

*Corresponding author.

693

stall on a conventional microscope which most medical institutions own. At the same time, we have to make sure that the price of this module is affordable, which makes us abandon the method of installing an auto-focus digital camera on top of the microscope. We, however, chose the Raspberry Pi High-Quality Camera as our image collector.

Such a choice has to pay the price: There is no auto-focus system in the pi camera; we have to control the adjustment wheel on the microscope with motors and take several photos while scrolling it. As a result, we'll get a set of images that involve different heights from the microscope stage to the microscope objective, which means we have to figure out the way to pick out the non-blurry image from the set. However, there were quite a few differences between the daily photos and cell images captured with a microscope. And that's the primary purpose of the algorithm we designed and implemented in this paper.

In Section 2, we introduce related works for microscope auto-focus. Section 3 describes our microscope image auto-focus method based on Colorful-Gradient and propose our Colorful-gradient auto-focus algorithm (CGAF). And we analyze the experimental results in Section 4. Finally, we conclude this paper in Section 5.

2 RELATED WORKS

In this section, we review several previous studies of focus measurement. We search for how people solve the blurry image filtering problem nowadays. A focus measure is a stated quantity used to calculate the pixel sharpness locally. Sharpness is a general term for every focus measurement score to be taken as a sharpness value. To calculate it, several focus operators are proposed by different researchers. In the research of Pertuz et al. (Pertuz et al., 2013), six main groups of sharpness operators were used in the work. We pick four of them as our competitors to evaluate our performance. The four sharpness operator groups are shown in the following lines.

1 **Gradient-Based Operators:** This group of focus measures uses the first image derivative or gradient to measure the focus level. Considering the images as a function f of the intensity value of $pixels(x, y)$, the gradient g can be computed by:

$$g = \sqrt{\left(\frac{\partial f}{\partial x}\right)^2 + \left(\frac{\partial f}{\partial y}\right)^2} \qquad (1)$$

This is also one of the most commonly used focus measurements. However, there is an assumption that this operator is based on: focused images present more sharp edges than blurred ones. This also means that it is pretty sensitive to the sharp edges in an image.

2 **Laplacian-Based Operators:** These operators are similar to the Gradient-based operator group. These focus measures are based on the second derivative of an image. Considering the images as a function f of the intensity value of $pixels(x, y)$, the Laplacian can be computed by the equation below, which is usually defined as divergence of the gradient of a function f:

$$\Delta f(x, y) = div(grad(f)) \qquad (2)$$

Group members such as Energy of Laplacian and Variance of Laplacian have been used as a focus measure for auto-focus in many pieces of research. A focus measure based on an alternative definition of the Laplacian, known as the modified Laplacian, showed the ability to become a focus measurement value (Nayar and Nakagawa, 1994). To conclude, Laplacian has shown a remarkable ability to deal with accurate shape recovery, making us later pick the Laplacian-based operator as our first experimental option.

3 **Wavelet-Based Operators:** These operators are based on the discrete wavelet transform coefficients. Thus, these coefficients are used to compute the focus amount of an image. However, these kinds of operators have primarily been based on the statistical properties of the discrete wavelet transform (DWT) coefficients. It is a focus measurement for auto-focus computing from the sub-bands of a higher-level discrete wavelet transform which is basically the sum of wavelet coefficients (Yang and Nelson, 2003).

4 **DCT-Based Operators:** This group of operators utilizes the discrete cosine transform coefficients to calculate the degree of focus. The discrete cosine transform is now part of many images and video encoding algorithms. The sum of the AC components of the DCT was proved to be equal to the variance of the image intensity and can be used as a focus measure (Baina and Dublet, 1995). Shen and Chen proposed a ratio between DC and AC components in the DCT as a new focus measurement method (Shen and Chen, 2006). Lee et al. applied the DCT to 8×8 image sub-blocks in order to measure focus (Lee et al., 2009). To improve the computation time, they picked only 5 out of 63 AC coefficients to compute the AC energy, which made the whole calculation faster and was named DCT reduced energy ratio.

Based on this literature review section, we started everything from the one with higher accuracy of

shape recovery, the Laplacian-based operator. However, we faced problems due to these high-accuracy features and the particular situation while processing microscopy images. Nonetheless, six different focus measurement operators are finally chosen as components in the simulation section. We will compare our method of this research to others while processing the same set of images.

3 METHODS

Picking a clear image is vital in our project. After placing one patient's blood samples onto the microscope stage, we control the stage's height with motors and get a cluster of images that contains photos with the variable focus of the same sample. Then, this cluster of images will transfer to our server to begin processing the clear image selection calculation. Finally, when we get a single most explicit image, we run our AI model to classify cells in the images and even analyze the image with pre-trained medical knowledge. The complete process can be finished while the medical personnel is having a nice sleep, and a detailed report will be shown on the user's computer at the end. However, in this research, we focus our methodology on the focus measurement instead of the whole microscope project.

Most auto-focus methods are based on a sharpness function that delivers a real-valued image quality estimate. However, a threshold has to be set to classify whether the target image is blurry or not. Meanwhile, the most commonly used method for filtering blurry images is the Gradient-based operator or Laplacian-based operator calculation of an image. As a result, in our early pipeline design, there was only one component: "calculate the sharpness value." After facing different problems, we devised a new pipeline solution for the microscope image focus measurement.

1 **Sharpness Measurement:** Using the second derivative of an image, we could get the areas of rapidly changing intensity in the image (Pech-Pacheco et al., 2000). The Laplacian operator is often used for edge detection. Furthermore, this algorithm is based on the assumption that if a picture has high variance, then it has a broader frequency response range, representing a typical, well-focused picture. But if the picture has a slight variance, it has a narrower frequency response range, which means that the number of edges in the picture is low. As we know, the blurrier the picture is, the fewer it has edges. At the beginning of our experiment, we thought it would be straightforward to pick a clear image since
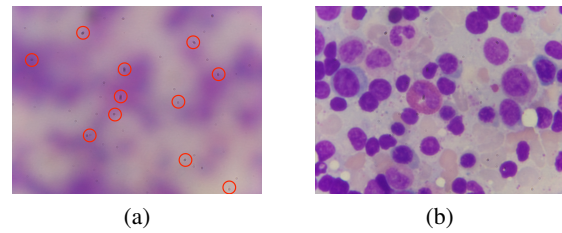

Figure 1: Fixing impurities on the microscope makes the program regard a blurry image as a clear image with several sharp edges of impurities target.

Laplacian-based operators have been regarded as the most effective way to get this job done. However, compared to the standard image in our daily life, there were too many impurities in the microscope image (Figure 1). Every impurity on the image will be recognized as several rapidly changing intensity areas. This would make the Laplacian transform value quite similar between photos since every image uses the same microscope lenses, and there will be the same impurities in the same position. The red circle in Figure 1(a) shows the impurities in the image. Figure 1(b) is the clear image of this set of images, which we expected the program to pick.

However, we still needed information on the sharpness value of the image. We then tried the Gradient-based operator, which only calculates the first derivative of the image. Formally, an image gradient is defined as a directional change in image intensity. Finally, we got a more accurate result compared to the Laplacian-based operator. Figure 2 illustrates the sharpness value calculated with both Laplacian and gradient-based operators, the clearest image in this set is the 35-th (image ids). In this figure, the x-axis coordinate shows the image of a set, which also stands for the different distances between the microscope stage and the microscope objective (descending power). The y-axis corresponds to the sharpness value of both Gradient-based and Laplacian-based operators.

2 **Colorfulness Measurement:** Although sharpness seems to be the most efficient method for blur detection, we found that since impurities are black dots of various sizes when the image is being transformed into grayscale in the sharpness calculation process, machines cannot tell the impurities or the cells are precisely the main targets it should focus on. This resulted in making the wrong decision about a clear image. We come up with a different aspect of blur detection in this case-Colorfulness calculation. The whole point of the colorfulness calculation is that we want to filter the total blur image with only
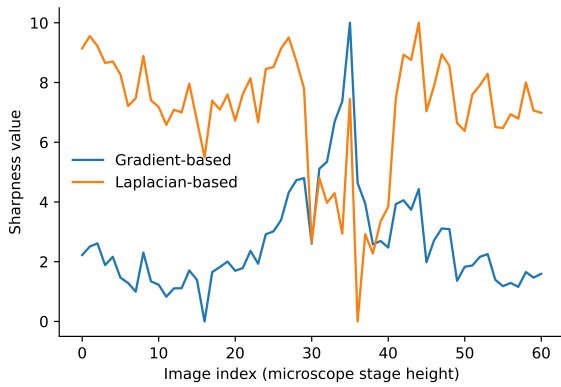
Figure 2: Comparison between Gradient-based sharpness value and Laplacian-based sharpness value.

impurities. These kinds of images share a common feature: they lack other colors except black and white. Haslera and Süsstrunk the colorfulness calculation (Haslera and Süsstrunk, 2003). First, they split the image into RGB color values, R, G, and B. Then, they immediately calculate

$$rg = R - G \qquad (3)$$

$$yb = \frac{1}{2R + 2G} - B \qquad (4)$$

Following up, they calculated both the standard deviation of rg, σ_{rg}, the standard deviation of yb, σ_{yb}, the mean value of rb, μ_{rb}, and the mean value of yb, μ_{yb}, to fit the final Colorfulness function

$$Colorfulness function = \sigma_{rgyb} + 0.3 \times \mu_{gryb} \quad (5)$$

where

$$\sigma_{rgyb} = \sqrt{\sigma_{rg}^2 + \sigma_{yb}^2} \qquad (6)$$

$$\mu_{rgyb} = \sqrt{\mu_{rg}^2 + \mu_{yb}^2} \qquad (7)$$

We set it as a double-check value which makes sure that the high sharpness of a single image is not just caused by the impurities on the microscope lenses. Figure 3 shows the difference between adding colorfulness to the sharpness value or not. The index of the image stands for the microscope stage's height, as when the index increase, the stage height goes higher and higher to the microscope objective. If the colorfulness value is not considered, the program will pick the second image as the clearest due to the impurity problem. On the other hand, colorfulness did help check this kind of mistake by making the correct clear image have a higher score by adding a higher colorfulness value on the sharpness value.

3 CIE Lab Color Space: Combining colorfulness and sharpness to calculate the focus value seems
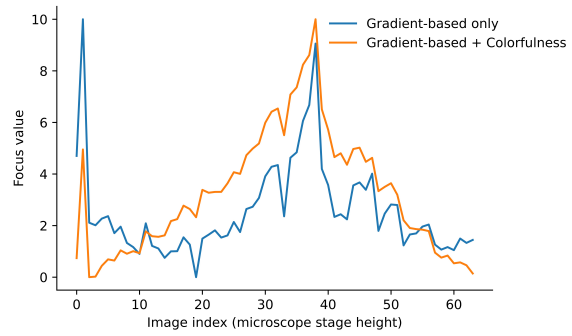

Figure 3: Showing how the colorfulness value helped in the situation of impurities problems.
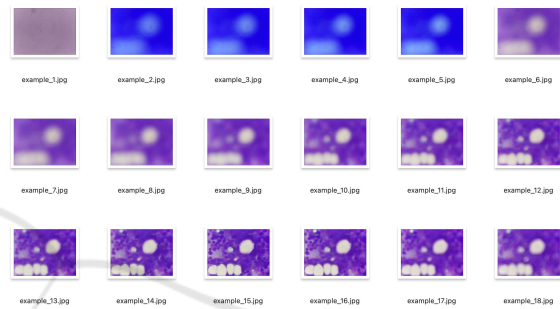

Figure 4: A general look of a set of images with a color cast problem.

to be the most accurate method to identify the clear microscope image. However, the illuminator under the stage can sometimes cause serious color cast problems, as shown in Figure 4. Noticed that it should be a set of images from blurry to non-blurry, but several of them suddenly had a color casting problem with a blue tone. Considering that we were using colorfulness as one of our central scoring values, the program may give a very high score to the color cast image in the aspect of colorfulness. As a result, we modified the colorfulness calculation function with CIE Lab color space to check for the image's color cast degree. The distance between colors in the color space is consistent with its perceived difference, so it is more reasonable to detect the color cast image under it.

4 Pipeline Processing: Finally, we designed a new process to solve the microscope image autofocus, considering that there will be undodgeable impurities on the lens and illuminator accidentally causing the color cast problem. As Figure 5 shows below, when an image is inputted to the operator, we will start calculating the sharpness value, colorfulness value, and color cast score parallelly. Afterward, we multiply the reciprocal number of the color cast score by the colorfulness value and
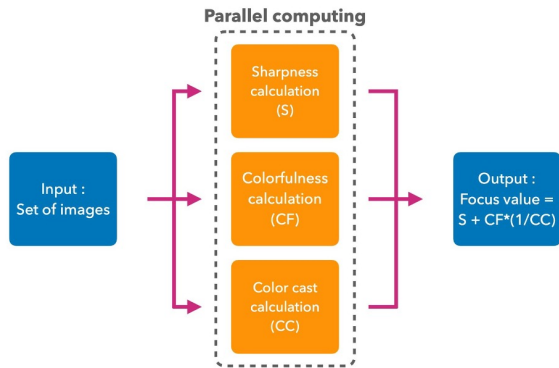
Figure 5: The overall workflow of the Color-gradient focus value calculation.

add the original sharpness value on it to get the final focus value of the colorful-gradient operator. Algorithm 1 shows the detail of our method. To begin, three lists will be declared (Sharpness, Colorful, ColorCast) for storing sharpness value, colorfulness value, and color cast score, respectively. Secondly, we read the image to the variable "im" to start calculating the three main components in three color-gradient functions (S, CF, CC) with three sub-functions (SCal, CCal, CCCal). After traversing the directory, we scale all the values with a min-max scaler and get the focus value with the proposed function. Finally, the index of the image with the highest focus value will return as an output.

4 EXPERIMENTAL RESULTS

To have a better look at the colorful-gradient operator's ability, we set up a few other operators to compare the performance of picking the non-blurry image from a set of images. The testing process included 18 directories of images, each of them containing multiple images from blurry to non-blurry images, which are all taken in real-life patients' blood samples. For these 18 cases of images, there are 12 cases taken on microscopes with impurities on the lens, and 6 cases are taken on a microscope with a clean lens. We compare our method, color gradient (C_g), with Gradient-based (G_b), Laplacian-based (L_b), wavelet summary (W_s), wavelet variance (W_r), DCT ratio (D_r), and DCT reduced ratio (D_{rr}). As Table 1 shows below, the colorful gradient is doing a great job in the 12 cases with impurities. The most explicit image in every case is accurately picked by it. However, most of the other operators could not have a stable performance while facing impurities problems. On the other hand, when it comes to cases without the interference of impuri-

---

Algorithm 1: Colorful-gradient auto-focus algorithm (**CGAF**).

Input: A list of strings (path of every image in the image directory), $Input = [path_1, path_2, path_3, \cdots, path_n]$.

Output: A index of the most explicit image.

```
1 begin
2    Sharpness ← [];
3    Colorful ← [];
4    ColorCast ← [];
5    len = length(Input);
6    while len > 0 do
7        im ← ImageToArray(Input[len − 1]);
8        Append SCal(im) to Sharpness;
9        Append CCal(im) to Colorful;
10       Append CCCal(im) to ColorCast;
11       len ← len − 1;
12   end
13   SS ← MinMaxScaler(Sharpness);
14   CS ← MinMaxScaler(Colorful);
15   CCS ← MinMaxScaler(ColorCast);
16   Focus ← ColorGradient(SS, CS, CCS);
17   return FindMaxValueIndex(Focus);
18 end
```

Table 1: The benchmark with impurity interference

# steps, s	C_g	G_b	L_b	W_s	W_v	D_r	D_{rr}
$s < 1$	12	6	2	1	7	5	0
$5 \leq s < 15$	0	3	3	1	1	5	5
$15 \leq s < 35$	0	0	0	1	0	0	2
$s \geq 35$	0	3	7	4	4	2	3

ties, as Table 2 showed, all of the operators can nearly pick the clearest image by an error of about three steps on average. We can still observe that the colorful-gradient operator is very stable, regardless of whether the impurities are interfering.

Not only can the colorful gradient handle the impurities cases, but it can also deal with a color cast that often happens in microscope images. One of the 12 cases with impurities interference also has a severe color casting problem, as shown in Figure 5 (Notice that to have an easier understanding of the color cast problem, we did not show all of the images in Figure 6. We picked images with an interval of three started from the fourth image). A standard microscope image of blood cells should be purple due to the dye fusing in the sample for more straight-

Table 2: The benchmark without impurity interference

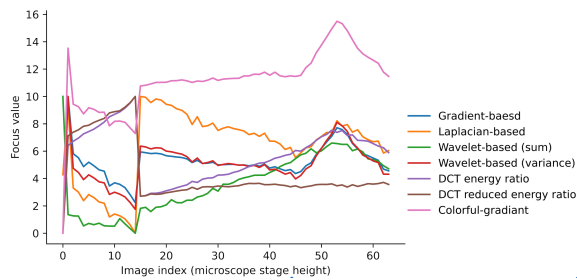| # steps, s	C_g	G_b	L_b	W_s	W_v	D_r	D_{rr}
$s < 1$	5	3	1	0	1	0	0
$5 \leq s < 5$	1	3	5	6	5	6	5
$s \geq 5$	0	0	0	0	0	0	1

Figure 6: Benchmark comparison between other operators and the Color-gradient operator.

forward observation. However, we can see several photos in the set have a color casting to blue (example_1 $\sim$ 5.jpg), which made all of the operators pick the example_2.jpg, which is the wrong one with the color cast problem. Figure 6 is a line chart of all the operators calculating this color cast case. Because of the blue color casting, all lines suddenly peak when the image index is number 2. Even if the process finally meets the actual clear image, number 52 in the set, the peak can only be a local maximum instead of a global maximum for all the other operators, leading to a wrong answer. Once again, the colorful gradient operator is still the only one that survives in this color casting case.

The final simulation with python code files is all open sources on the internet. Please refer to the URL: https://github.com/Pockylee/Colorful-gradient for a deeper understanding of the colorful-gradient operator algorithm.

5 CONCLUSIONS

We proposed a new focus measurement operator considering three aspects: sharpness, colorfulness, and color cast. Unlike most sharpness operators nowadays, colorful-gradient cannot only do the regular image focus measurement job well, but it can also easily deal with microscopy cases. According to the real-life data collected from medical institutes, we found the two main factors of making microscopy images harder to do focus measurement. First, the impurity on the lens is an undodgeable problem, especially in medical institutions located in remote areas. Second, the color cast problems are caused by the illuminator of a conventional microscope. After all, we tested the operators with real-life data and constructed a benchmark to show the difference between the colorful-gradient operator and others. With the focus algorithm we propose, we can perform excellently on the microscope image focus detection cases. We had already implemented this algorithm onto the automated

microscope system. However, the current algorithm is not fast enough to make a real-time adjustment with the microscope stage adjust wheel. We can only take one photo on every slight rotation (step) of the adjustment wheel; after gathering all of the images of the sample, we send them to the server to find the perfect height for the microscope stage. As a result, we can start from a higher height instead of taking the photo from the bottom, which wastes much time.

REFERENCES

Baina, J. and Dublet, J. (1995). Automatic focus and iris control for video cameras. In *Fifth International Conference on Image Processing and its Applications*, pages 232–235.

Blixt, L., Bogdanovic, G., Buggert, M., Gao, Y., Hober, S., Healy, K., Johansson, H., Kjellander, C., Mravinacova, S., Muschiol, S., Nilsson, P., Palma, M., Pin, E., Smith, C. I. E., Stromberg, O., Chen, M. S., Zain, R., Hansson, L., and Österbor, A. (2022). Covid-19 in patients with chronic lymphocytic leukemia: clinical outcome and b- and t-cell immunity during 13 months in consecutive patients. *Leukemia*, 36(2):476–481.

Haslera, D. and Süsstrunk, S. (2003). Measuring colourfulness in natural images. In *SPIE - the International Society for Optical Engineering*, volume 5007, pages 87–95.

Lee, S.-Y., Yoo, J.-T., Kumar, Y., and Kim, S.-W. (2009). Reduced energy-ratio measure for robust autofocusing in digital camera. *IEEE Signal Processing Letters*, 16(2):133–136.

Nayar, S. K. and Nakagawa, Y. (1994). Shape from focus. *IEEE Transactions on Pattern Analysis and Machine Intelligence*, 16(8):824–831.

Pech-Pacheco, J. L., Cristobal, G., Chamorro-Martinez, J., and Fernandez-Valdivia, J. (2000). Diatom autofocusing in brightfield microscope: a comparative study. In *the 15th International Conference on Pattern Recognition (ICPR-2000)*, volume 3, pages 314–317.

Pertuz, S., Puig, D., and Garcia, M. A. (2013). Analysis of focus measure operators for shape-from-focus. *Pattern Recognition*, 46:1415–1432.

Shen, C.-H. and Chen, H. H. (2006). Robust focus measure for low-contrast images. In *2006 Digest of Technical Papers International Conference on Consumer Electronics*, number 69-70.

Tong, X., Cheng, A., Yuan, X., Zhong, X., Wang, H., Xu, W. Z. X., and Li, Y. (2021). Characteristics of peripheral white blood cells in covid-19 patients revealed. *BMC Infectious Diseases*, 21(1):1236.

Yang, G. and Nelson, B. J. (2003). Wavelet-based autofocusing and unsupervised segmentation of microscopic images. In *2003 IEEE/RSJ International Conference on Intelligent Robots and Systems (IROS 2003) (Cat. No.03CH37453)*, pages 2143–2148.